Polyion Complex Nanomaterials from Block Polyelectrolyte Micelles and Linear Polyelectrolytes of Opposite Charge. 2. Dynamic Properties

Pavel S. Chelushkin,[†] Evgeny A. Lysenko,[†] Tatiana K. Bronich,[‡] Adi Eisenberg,[§] Victor A. Kabanov,[#] and Alexander V. Kabanov*,[†,‡]

Department of Polymer Sciences, Faculty of Chemistry, M.V. Lomonosov Moscow State University, Leninskie Gory, V-234, Moscow, 119991, Russia, Department of Pharmaceutical Sciences and Center for Drug Delivery and Nanomedicine, College of Pharmacy, University of Nebraska Medical Center, 986025 Nebraska Medical Center, Omaha, Nebraska 68198-6025, and Department of Chemistry, McGill University, 801 Sherbrooke Street West, Montreal, Quebec, Canada H3A 2K6

Received: February 13, 2008; Revised Manuscript Received: March 25, 2008

The present study investigates the relationship between the aggregation state and dynamic properties of block ionomer complexes (BICs) based on amphiphilic ionic block copolymers. The polyion coupling of 4′-(aminomethyl)fluorescein (AMF)-labeled poly(sodium methacrylate) (PMANa) or polystyrene-*block*-poly(sodium carboxylates) with poly(*N*-ethyl-4-vinylpyridinium bromide), PEVP was studied at an excess of carboxylate groups $[PEVP]/[COO^-]_{TOTAL} = 0.3$ and detected by fluorescence quenching. The polyion interchange reactions included migration of PEVP between the following: (1) two linear polyanion chains, (2) linear polyanion chain and anionic polyion shell micelle, or (3) two anionic polyion shell micelles. Additionally, the interchange of AMF-labeled PMANa with unlabeled PMANa in the shell of polystyrene-*block*-PEVP micelles was studied. The interchange reactions were carried out at $[PEVP]/[COO^-]_{TOTAL} = 0.15$ and detected by fluorescence quenching (direct reaction) or ignition (reverse reaction). The rates of these reactions were compared using half-conversion times and, when possible, second-order reaction kinetic constants. The dependences of the rates on the ionic strength and polyion length observed for BICs were similar to those previously reported for regular interpolyelectrolyte complexes (IPECs) of linear polyions. However, the interchange reactions involving polyion shell micelles were much slower than those reactions observed in IPECs. The coupling reactions involving polyion shell micelles were also slower compared with the coupling of linear polyions. The observed phenomena were attributed to the aggregation state of polyion shell micelles and discussed using the collision model for polyion interchange reactions previously proposed for IPECs.

Introduction

Block ionomer complexes (BICs) are formed as a result of the interaction of block polyelectrolytes with oppositely charged low-molecular-mass amphiphilic surfactants, synthetic polyions, or biopolymers.[1,2] They are hybrid materials displaying environmental sensitivity of ordinary interpolyelectrolyte complexes (IPECs)[3–5] and core−shell architecture of block copolymer micelles.[6,7] Water-soluble BICs with a polyion complex core and nonionic hydrophilic polymer shell have found application in delivery of DNA, proteins, and drugs.[8–11] The present study focuses on a different, relatively new type of BIC, which is synthesized by reacting linear polyelectrolytes with oppositely charged block polyelectrolyte micelles having a hydrophobic core and polyion shell. Such polyion shell micelles (PSMs) are composed of amphiphilic block copolymers containing a nonionic hydrophobic block and a polyion block, such as polystyrene-*block*-poly(sodium carboxylates) or polystyrene-*block*-poly(*N*-ethyl-4-vinylpyridinium bromide) (PS-*b*-PEVP). Interaction of PSMs with oppositely charged linear polyelectrolytes, such as PEVP or poly(sodium carboxylates), can lead to formation of water-soluble nanosized complexes.[12–19] Such complexes have a multilayer structure with a hydrophobic nonionic core, intermediate water-insoluble polyion complex layer, and surrounding hydrophilic shell of the excessive polelectrolyte.[12–18]

Previous work[19] has studied the dispersion stability of such BICs in aqueous media as a function of the composition and chemical nature of the reacting polyelectrolytes. It was shown that at an excess of the linear polyelectrolyte BIC behaved similar to regular IPEC. In particular, soluble BIC formed only if the linear polyelectrolyte formed soluble IPEC with another linear polyelectrolyte having the same chemical nature as the shell-forming block of the PSM. In contrast, at an excess of the PSM, stable dispersions of the BIC could be obtained independently of the chemical nature of reacting polyelectrolytes, even in the cases when soluble IPEC did not form. Interestingly, at an excess of PSM, soluble complexes can be formed not only by synthetic linear polyelectrolytes but also by proteins that bind in the polyion shell of the micelles.[20] Such BICs are of potential interest for applications in biomaterials and other fields.

One essential property of regular IPECs is their ability to participate in highly cooperative polyion interchange reactions

* To whom correspondence should be addressed. Fax: (402) 559-9365. E-mail: akabanov@unmc.edu.
† Department of Polymer Sciences, Faculty of Chemistry, M.V. Lomonosov Moscow State University.
‡ Department of Pharmaceutical Sciences and Center for Drug Delivery and Nanomedicine, College of Pharmacy, University of Nebraska Medical Center.
§ Department of Chemistry, McGill University.
# Deceased.

10.1021/jp8012877 CCC: $40.75 © 2008 American Chemical Society
Published on Web 06/06/2008

SCHEME 1: Structure of Polymers

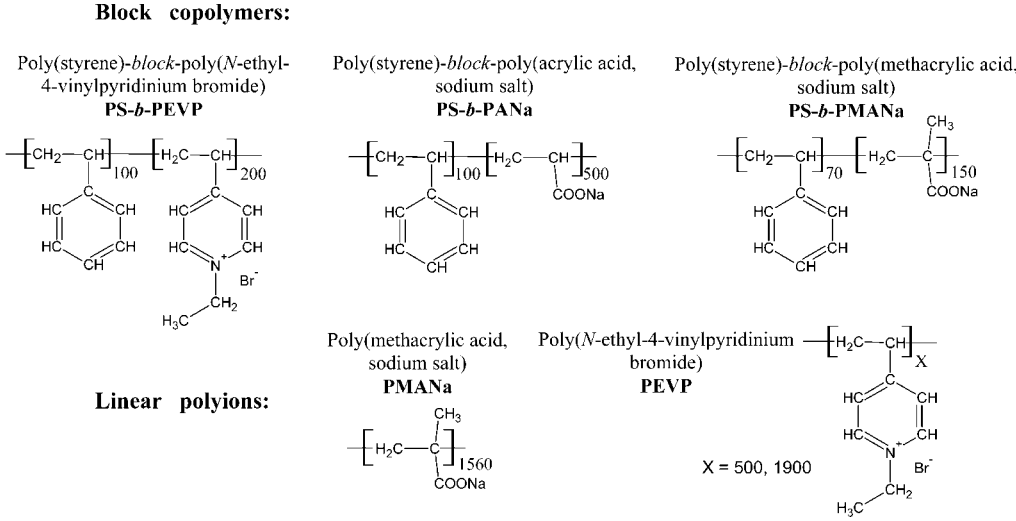

with other polyelectrolyte components present in solution.[4] However, as of today, little is known about such reactions involving BICs.[21–23] Furthermore, the kinetics of polyion coupling of PSM and linear polyelectrolytes was not explored. This deficiency is addressed by the present study using a fluorescence technique to determine the rates and directions of the polyion coupling and interchange reactions involving PSM. The study focuses on soluble BICs formed at an excess of PSM and compares the results with the behavior of regular IPECs. Overall, this study shows that aggregation of block polyelectrolytes into PSM drastically decreases the rates of polyion coupling and interchange reactions compared to similar reactions of linear polyelectrolytes.

Experimental Section

Materials. Ethyl bromide (EtBr, 98%, Aldrich Chemical Co., Inc., Milwaukee, WI) and *N*,*N*-dimethylformamide (DMF, reagent for molecular biology, Sigma-Aldrich, Inc., St. Louis, MO) were used without further purification. All aqueous solutions were prepared, and all dialyzes were performed with type 1 water purified by WaterPro PS 90007-00 model (Labconco Co., Kansas City, MO). Chemical structures of all polymers are shown in Scheme 1.

Block Copolymers. Block copolymer of styrene and *N*-ethyl-4-vinylpyridinium bromide (PS(100)-*b*-PEVP(200), here and below, numbers in parentheses correspond to weight-average polymerization degrees (DP_w) of the blocks) was synthesized as follows. First, the block copolymer of styrene and 4-vinylpyridine (PS(100)-*b*-PVP(200)) was synthesized by sequential anionic polymerization.[24] The polydispersity index (M_w/M_n ratio) of the resulting block copolymer was about 1.12. After that, PS(100)-*b*-PEVP(200) (further designated as PS-*b*-PEVP) was obtained by exhaustive quaternization of PVP block by EtBr.[25] The degree of modification of the poly(4-vinylpyridine) (PVP) block was not less than 90% as determined by IR spectroscopy. Aqueous dispersions of PS-*b*-PEVP were prepared using the dialysis technique as described earlier.[25] The concentration of PS-*b*-PEVP after dialysis was determined using UV-spectrophotometry technique.

Block copolymer of styrene and acrylic acid, PS(100)-*b*-PAA(500) (designated as PS-*b*-PAA), was synthesized by sequential anionic polymerization of styrene and *tert*-butylacrylate followed by exhaustive hydrolysis of *tert*-butylacrylate block as described before.[26] The polydispersity index of the resulting block copolymer was about 1.12. Aqueous dispersions of PS-*b*-PAA were prepared using the dialysis method as described earlier.[19]

Block copolymer of styrene and methacrylic acid (PS(70)-*b*-PMAA(150)) (further designated as PS-*b*-PMAA) was purchased from Polymer Source, Inc. (Montreal, Canada). The polydispersity index was 1.13. Preparation of aqueous dispersions of PS-*b*-PMAA and its sodium salt PS-*b*-PMANa was similar to the procedure for PS-*b*-PAA.

Linear Polyelectrolytes. Poly(methacrylic acid) (PMAA) ($DP_w = 1560$) was synthesized via radical polymerization and fractionated as described previously.[17] Poly(sodium methacrylate) (PMANa) was obtained by neutralization of aqueous PMAA solutions by NaOH. PVP samples ($DP_w = 500$, 1900; Polysciences, Inc., Warrington, PA) were exhaustively modified by EtBr to obtain PEVP.[25] The modification degree was 90%.

Fluorescent Labeling of Polymers. PS-*b*-PAA was labeled with a fluorescent label (4′-(aminomethyl)fluorescein hydrochloride (AMF), Molecular probes, Eugene, OR) using a modified procedure.[27] A detailed description of this procedure is given in our previous publication.[19] Labeling density measured by combination of potentiometric titration and UV spectrophotometry was 1 label per 5100 carboxylic groups in the case of PS-*b*-PA*A, 1 label per 3700 carboxylic groups in the case of PS-*b*-PMA*A, and 1 label per 900 carboxylic groups in the case of PMA*A (here and below, labeled polymers are designated by the asterisk symbol). Aqueous dispersions of PS-*b*-PA*A or PS-*b*-PMA*A micelles or their sodium salts (PS-*b*-PA*Na or PS-*b*-PMA*Na) were prepared following the procedure described above for unlabeled samples.

UV Measurements. Molar concentrations of pyridinium units in PEVP solutions or PS-*b*-PEVP dispersions were calculated from their absorbance at 257 nm (molar absorption coefficient is 3000 $L \cdot mol^{-1} \cdot cm^{-1}$).[28] UV spectra were recorded on a UV−vis spectrophotometer, Lambda-25 (Perkin-Elmer, Wellesley, MA), in 10 mm quartz cells.

Dynamic Light Scattering (DLS). Prior to all light scattering measurements, the samples were filtered 2−3 times through Millipore GS 0.45 μm filters. DLS experiments were performed on a FotoKorr-M 72-channel correlator at a scattering angle of 90°. Diffusion coefficients (D_z) were calculated by a cumulant analysis of an autocorrelation function of scattered light intensity fluctuations. Effective hydrodynamic radii (R_h) were calculated from diffusion coefficients using the Stokes equation:

$$D_z = \frac{k_B T}{6\pi\eta R_h} \quad (1)$$

where k_B is the Boltzmann constant, T is absolute temperature, and η is the intrinsic viscosity of a solvent. For all measurements of D_z, the experimental error did not exceed 5%.

Static Light Scattering (SLS). Molecular mass measurements were carried out with a scattered laser light goniometer, FotoCorr Complex (FotoCorr Instruments, USA) at 25 °C and a scattering angle of 6−7°. A 25-mW He−Ne laser operating at 633 nm wavelength was used as the light source. SLS data processing was performed using toluene as a reference. Refractive index increments used to determine the optical constant K were measured by a KMX-16 differential refractometer (Milton Roy, USA) with a 0.5-mW He−Ne laser as a light source. Solvent equilibrated by dialysis with solution under investigation was used as the reference sample. Weight-averaged aggregation numbers of macromolecules per micelle, N_w, were calculated as the ratio M_w/M_0 where M_w and M_0 are molecular masses of an aggregate and single block copolymer, correspondingly.

Fluorescence Measurements. Fluorescence time scans were recorded using a Cary Eclipse fluorescence spectrophotometer (Varian, Inc., Palo Alto, CA) at $\lambda_{EX} = 490$ nm and $\lambda_{EM} = 520$ nm with a bandwidth of 2.5 nm for excitation and 5 nm for emission. All measurements were performed at room temperature and processed using software provided by the manufacturer.

Results and Discussion

Stoichiometric complexes of oppositely charged polyelectrolytes are usually water insoluble and precipitate.[4,29] Nonstoichiometric complexes can be soluble depending on the chemical nature of reacting polyelectrolytes. For example, various BICs of PSM and linear polyelectrolytes can form stable aqueous dispersions if one of the polyelectrolyte components is present at a certain excess.[19] We and others have shown that under such conditions nonstoichiometric BIC are formed, which have a multilayer structure with a hydrophobic nonionic core, insoluble polyion complex layer, and hydrophilic shell of the excessive polyelectrolyte.[12–18]

It was of interest to compare such complexes with soluble nonstoichiometric IPEC formed by linear homopolymers.[4] Unlike BICs, nonstoichiometric IPECs usually do not form core−shell aggregates. They often contain one longer polyelectrolyte chain present in excess, which is partially neutralized by one or several shorter chains of opposite charge. The polyelectrolyte present in excess provides for solubility of the nonstoichiometric IPEC. It is called Host Polyelectrolyte (HP), while the oppositely charged polyelectrolyte is called Guest Polyelectrolyte (GP). Formation and rearrangement of nonstoichiometric IPEC proceed through highly cooperative reactions of polyion coupling (I) and polyion interchange (II):

$$GP + HP = \{GP/HP\} \quad (I)$$

$$\{GP/HP_1\} + HP_2 = HP_1 + \{GP/HP_2\} \quad (II)$$

(Here and below the complexes are designated by brackets "{}".) If HP_1 and HP_2 are identical, then the reaction (II) is called a polyion exchange.[30] If HP_1 and HP_2 are different, then the process is called a polyion substitution reaction.[31] As demonstrated by Bakeev et al.,[30] the polyion coupling reaction (I) proceeds through a complex mechanism involving a sequence of progressive polyion exchange reactions (II).

We hypothesized that nonstoichiometric BICs of PSM and linear polyelectrolytes can also participate in such reactions. We further suggested that the kinetic behavior of the reactions involving BICs and ordinary IPEC may differ significantly due to the effect of the polyion shell in PSM. Of particular interest are the conditions of the PSM excess, because in this case the polyion interchange (and coupling) should involve polyion migration into the PSM shell. To evaluate our hypotheses, we compared the processes of polyion migration in the systems containing PSM with similar reactions in the systems containing linear polyelectrolyte coils of the same chemical nature of ionic units. The PS-*b*-PANa and PS-*b*-PMANa micelles or PMANa homopolymer were used as HP components. The PS-*b*-PEVP micelles or PEVP homopolymer were used as the GP components. The chemical structures of all polymers are shown in Scheme 1. The molecular characteristics of PSM are summarized in Table 1. The PSM had hydrodynamic radii ranging from 26 to 43 nm and contained from about 38 to about 160 macromolecules per micelle. For the fluorescence detection, the polyanions were tagged with AMF labels, which were quenched upon binding of the PEVP chains. We assumed that due to very low density of AMF tags in labeled PS-*b*-PA*Na and PS-*b*-PMA*Na the molecular characteristics of the labeled and unlabeled PSM were the same. (The labeled polymers are designated herein by the asterisk " * ".)

TABLE 1: Molecular Characteristics of Block Copolymer Micelles in Aqueous Media[a].

block copolymer	$M_w \cdot 10^{-6}$, g/mol	N_w	R_h, nm	[ionic groups]$_{shell}$, M
PS-*b*-PEVP	2.02	38	26	0.18
PS-*b*-PMANa	3.64	160	43	0.12
PS-*b*-PANa	1.92	41	36	0.17

[a] Weight-averaged molecular mass (M_w), weight-averaged aggregation number of macromolecules per micelle (N_w), hydrodynamic radius (R_h), and average concentration of ionic units in a micelle shell ([ionic groups]$_{shell}$); [NaCl] = 0.1 M.

The reaction conditions were chosen to avoid phase separation. We have shown earlier that each polycation/polyanion pair in this study can form stable aqueous dispersions at an excess of anionic component within the composition range $Z = [Py^+]/[COO^-]$ varying from 0 to 0.3.[19] The polyion coupling reactions were studied at $Z = 0.3$, and the polyion interchange reactions were studied at $Z = 0.15$ (initial complexes with $Z = 0.3$ were mixed with the equivalent of free polyions). For all of the reactions, a pH = 10 was used to obtain fully neutralized polyions (for interchange reactions performed at [NaCl] = 0.05 or 0.1 M, we used 0.01 M TRIS buffer; for coupling reactions performed at [NaCl] = 0.01 M, we adjusted the pH by NaOH). The following will be discussed separately: (1) polyion interchange reactions and (2) polyion coupling reactions.

Polyion Interchange Reactions. The following interchange reactions were studied. First, the migration of a relatively short linear cationic GP, PEVP, between two anionic HPs: (a) two linear PMANa coils, (b) PMANa coil and PS-*b*-PMANa micelle, and (c) two identical PS-*b*-PANa or PS-*b*-PMANa micelles. Second, the exchange of PMANa chains between BIC{PS-*b*-PEVP/PMANa} and external solution. In all experiments, an aliquot of a free polyion solution ($Z = 0$) was mixed with an aliquot of a complex solution with $Z = 0.3$. Both aliquots were of equal volume and had equal base molar concentrations of carboxylate groups. The final mixture compositions were $Z_{TOTAL} = [Py^+]/[COO^-]_{TOTAL} = 0.15$, where $[COO^-]_{TOTAL} = [COO^-]_{FREE\ POLYION} + [COO^-]_{COMPLEX}$.

Each reaction was studied in two directions. The "direct" process involved addition of AMF-labeled polyanion to complexes of unlabeled polyanion and polycation:

$$\{GP/HP_1\} + HP^*_2 = \{GP/HP^*_2\} + HP_1 \quad (IIa)$$

This resulted in fluorescence quenching due to the transfer of PEVP chains (fluorescence quencher) to the labeled polyanion (Figure 1, curves 1−3). The "reverse" process involved addition of unlabeled polyanion to complexes of labeled polyanion and PEVP:

$$\{GP/HP^*_2\} + HP_1 = \{GP/HP_1\} + HP^*_2 \quad (IIb)$$

This resulted in a fluorescence increase due to transfer of quencher to unlabeled polyanion chains (Figure 1, curves 1′−3′).

Data were plotted as the time dependencies of the "reduced fluorescence intensity", $I_R = (I - I_{MIN})/(I_{MAX} - I_{MIN})$, where I is the fluorescence intensity of the reaction mixture at any given time point, I_{MAX} is the fluorescence intensity of free polyanion HP^*_2, and I_{MIN} is the fluorescence intensity of the complex $\{GP/HP^*_2\}$ (Figure 1).[32] (In this representation, for all direct reactions (IIa) $I_R = 1$ at the initial mixing point and then gradually decreases to its equilibrium value, $I_{R(EQ)}$. In contrary, for all reverse reactions (IIb), $I_R = 0$ at the mixing and then increases to $I_{R(EQ)}$.) The conversion of the reaction, θ, equals I_R/I_{EQ} for the reverse reaction (IIb) and $(1 - I_R)/(1 - I_{EQ})$ for the direct reaction (IIa).

From Figure 1, one can notice that migration of PEVP chains between labeled and unlabeled polyanions proceeds with different rates in PMANa/PMA*Na, PMANa/PS-*b*-PMA*Na, and PS-*b*-PMANa/PS-*b*-PMA*Na systems. For quantitative comparison of reaction rates, we used two parameters, the half-conversion time, $\tau_{1/2}$, and the kinetic constant k.[4] The $\tau_{1/2}$ value was simply determined from the time dependence of I_R (Figure 1) as the time point, when $\theta = 0.5$. Notably, $\tau_{1/2}$ is not a characteristic kinetic parameter, since its value may depend on the concentration of reagents. However, $\tau_{1/2}$ allows comparison of the reaction rates as a whole. This parameter is applicable to reactions with complicated mechanisms, including polychronic interchange reactions, where the composition of reagents and reaction rate continuously change as the conversion degree changes.[4]

The kinetic constant (k) enables the most accurate comparison of reaction rates, but its determination for polyion interchange reactions is possible only in simple cases. One such case that has been previously described is the migration of one PEVP chain from its IPEC with PMANa chain onto a free pyrenyl labeled PMA*Na.[30] In this case, the reaction rate obeys the kinetic equation of a second-order irreversible reaction and hence, can be characterized by the second-order kinetic constant, k_{II}:

$$\frac{\theta}{1-\theta} = k_{II} \cdot C_0 \cdot t \quad (2)$$

where θ is conversion, C_0 is the initial concentration of PMANa, equal to initial concentration of PMA*Na, and t is time.

According to ref 30, the second order of the reaction is due to formation of a short-living intermediate ternary complex (PMANa···PEVP···PMA*Na) resulting from interpenetration of the initial IPEC and PMA*Na coils upon their random collisions in the solution ("collision mechanism"). This intermediate complex acts as a "transition state" in which the PEVP chain, through segmental mobility of its units, "chooses" the original or added polyanion. Theoretical and experimental studies showed that there are no free PEVP chains released in solution under the conditions of reaction (II).[4] Therefore, this reaction cannot proceed through dissociation of original IPEC onto macromolecular components with subsequent recombination of the released polycation with the added polyanion.

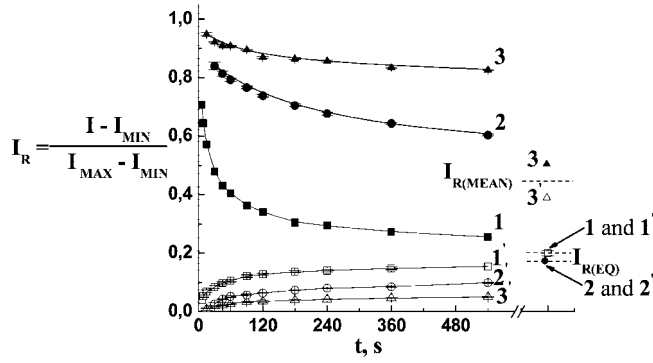

Figure 1. Kinetic curves (reduced fluorescence intensity vs time) for PEVP(500) exchange and substitution reactions with participation of PMANa and PS-*b*-PMANa: (1) PMA*Na + {PMANa/PEVP} = {PMA*Na/PEVP} + PMANa; (1′) {PMA*Na/PEVP} + PMANa = {PMANa/PEVP} + PMA*Na; (2) PS-*b*-PMA*Na + {PMANa/PEVP} = {PS-*b*-PMA*Na/PEVP} + PMANa; (2′) {PS-*b*-PMA*Na/PEVP} + PMANa = PS-*b*-PMA*Na + {PMANa/PEVP}; (3) PS-*b*-PMA*Na + {PS-*b*-PMANa/PEVP} = {PS-*b*-PMA*Na/PEVP} + PS-*b*-PMANa; (3′) {PS-*b*-PMA*Na/PEVP} + PS-*b*-PMANa = PS-*b*-PMA*Na + {PS-*b*-PMANa/PEVP}. [NaCl] = 0.05 M; pH 10 (0.01 M TRIS buffer); $[COO^-]^* = [COO^-] = 5 \times 10^{-4}$ M; $[Py^+] = 1.5 \times 10^{-4}$ M.

If the polyion complex contains several GP chains, then reaction 2 becomes polychronic with k_{II} being a function of θ. In this case, the initial rate of the reaction can be characterized by the kinetic constant $k_{II(0)}$, defined according to eq 2 as k_{II} at an infinitely low conversion degree ($\theta \rightarrow 0$). This approximate constant corresponds to the migration of the first GP chain between the complex particle and free polyanion.

We made an assumption that the mechanism of polyion interchange reactions involving PSM is similar to that described above for linear polyions. Specifically, the reaction involves reproaching and interpenetration of a free HP chain/micelle and the complex particle with formation of a ternary transition complex (e.g., (PMA*Na···PEVP···PS-*b*-PMANa) or (PS-*b*-PMANa···PEVP···PS-*b*-PMA*Na)), followed by a transfer of GP chains from one HP to another.

Two considerations support this assumption. The first one is the absence of free PEVP chains (GP) in aqueous dispersions of PS-*b*-PMANa or PS-*b*-PANa micelles, established via sedimentation velocity experiments in our previous publication.[19] (The absence of PEVP chains was also reported by Pergushov et al. for BICs of polyisobutylene-*block*-PMANa micelles and PEVP chains.[14]) Similar to the case of PMANa coils, this observation allows us to exclude the dissociation−recombination mechanism in reaction (II). The second consideration is that BIC have multilayer structure, that is, the PS core is surrounded by the intermediate insoluble layer of mutually neutralized polyions and the lyophilizing shell of the polyanion present in excess. On the basis of this structure, we posit that interpenetration of a negatively charged BIC particle and polyanion coil (or another PSM) and formation of a tertiary transition complex is the rate limiting stage of reaction (II).

To determine k_{II} or $k_{II(0)}$, we plotted original kinetic data in coordinates $\theta/(1 - \theta)$ vs t (Figure 2) and calculated k_{II} or $k_{II(0)}$ using eq 2 (here, C_0 is the initial concentration of kinetically independent particles of the free polyions, i.e., micelles or coils). The kinetic parameters for all reactions, studied in the paper, are summarized in Table 2.

On the basis of the kinetic data, the reactions were separated into three distinct groups. The first group included the fastest reactions (Figure 1, curves 1 and 1′), which proceeded within seconds at 0.1 NaCl (Table 2). This group included migration

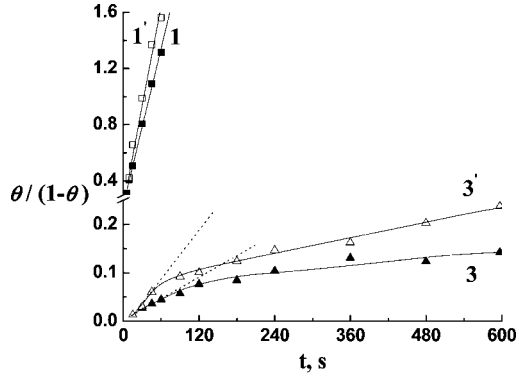

Figure 2. Kinetic curves plotted in second-order reaction coordinates ($\theta/(1-\theta)$ vs time, where θ is conversion) for PEVP(500) exchange reactions between PMANa or PS-*b*-PMANa (reactions 1, 1′, 3, and 3′ in Figure 1). [NaCl] = 0.05 M; pH 10 (0.01 M TRIS buffer); $[COO^-]^* = [COO^-] = 5 \times 10^{-4}$ M; $[Py^+] = 1.5 \times 10^{-4}$ M.

of PEVP between PMANa and PMA*Na coils and was depicted as "coil/coil" or "c/c". The kinetic curves corresponding to these reactions were linear in the coordinates $\theta/(1-\theta)$ vs t (Figure 2, curves 1 and 1′). This was consistent with the fact that at the mixing composition ($Z = 0.15$) one GP molecule was bound to one HP (or HP*).

The second group included slower reactions, which proceeded within dozens of seconds at 0.1 NaCl (Table 2). Because of the inequality of initial HP concentrations, kinetic constants for this reaction cannot be calculated from eq 2. This group included (i) migration of PEVP between PMANa coils and PS-*b*-PMANa micelles and (ii) PMANa exchange between BIC {PS-*b*-PEVP/PMANa} and external solution (Table 2). It was depicted as "coil/micelle" or "c/m". In the case of PEVP migration between PMANa and PS-*b*-PMANa, two processes were investigated: (a) direct and reverse migration of PEVP between PMA*Na and PS-*b*-PMANa and (b) direct and reverse migration of PEVP between PMANa and PS-*b*-PMA*Na. The only difference between these processes is the location of a label. Table 2 contains data on the process b alone, since kinetic parameters of both reactions were similar.

The third group included the slowest reactions (Figure 1, curves 3 and 3′), which proceeded within thousands of seconds at 0.1 NaCl (Table 2).[33] Since these reactions are polychronic (1 PSM binds on average 15 PEVP chains), these reactions formally do not obey the second-order kinetics. However, the values of $k_{II(0)}$ can be estimated using the initial slopes of the curves. Notably, the linear area extended up to 5 to 7% conversions, which corresponded to the transfer of approximately one polyion chain per the complex particle. Evidently, subsequent nonlinearity was due to the multichain migration. Because of slow rates the reactions did not reach equilibrium state. Therefore, we used $I_{R(MEAN)}$ (arithmetical mean between I_R of direct and reverse reaction after two months) instead of $I_{R(EQ)}$ to calculate $\tau_{1/2}$ and $k_{II(0)}$ values (Figure 1). This limitation may have contributed to the observed discrepancy of the $\tau_{1/2}$ values for direct and reverse reactions. This group included PEVP migration between labeled and unlabeled PS-*b*-PMANa or PS-*b*-PANa micelles and was depicted as "micelle/micelle" or "m/m".

Altogether, two major observations can be made based on these kinetic data. First, PEVP migration between two micelles has the same features as PEVP migration between two linear polyions: the reaction rate increased as the polymerization degree of PEVP decreased or the [NaCl] increased (Table 2, see ref 30 for exhaustive data on these effects for IPECs). Second, reaction rates decreased in the following order:

$$\text{coil/coil} > \text{coil/micelle} > \text{micelle/micelle} \qquad (3)$$

The phenomenon of slowing down the rate of interchange reactions in PSM-containing systems can be satisfactorily explained within the "collision" model postulated above.[30] The dependence of the reaction rate on the polymerization degree of GP (PEVP, in our case) and [NaCl] concentration in the case of micelles (Table 2) indirectly supported this mechanism. Indeed, since the shell of the PSM has much greater density of ionic groups compared to single polyion coils, the electrostatic and steric repulsion upon the reproaching and interpenetration of reacting species in the case of c/m and especially m/m is also much greater in comparison with c/c systems. This should result in a decrease of the rate of the polyion interchange reaction involving PSM.

In support of this hypothesis, we estimated the mean ionic group concentrations within the PS-*b*-PMANa micelle shell, $[COONa]_{shell} \sim 0.12$ M, based on the combination of DLS and SLS data.[35] This estimation is in reasonable agreement with similar estimations for other block copolymers (Table 1) and calculations based on neutron scattering.[36] At the same time, the mean ionic group concentrations within PMANa coils, estimated from crossover concentration was 0.024 M (both estimations were done for fully neutralized polyions at [NaCl] = 0.1 M). On this basis, it is reasonable to conclude that mutual penetration effectiveness will decrease in the following order: coil/coil > coil/micelle > micelle/micelle, and this is in good agreement with the observed experimental data (Table 2).

A similar situation probably arises in the case of PMANa exchange in {PS-*b*-PEVP/PMANa} BICs at an excess of PMANa. At $Z = 0.15$, the free PMANa coils coexist with the BIC particles having multilayer structure and PMANa chains in the outer shell. Therefore, the exchange process consists of reproaching and interpenetration of the PMANa chain through a PMANa-based shell followed by the transfer of the PEVP chains of PSM from one HP to another. This process is

TABLE 2: Second-order Reaction Constants (k_{II}) and Half-conversion Times ($\tau_{1/2}$) for Exchange and Substitution Reactions[a]

			$k_{II} \cdot 10^{-4}$, $M^{-1} \cdot s^{-1}$		$\tau_{1/2}$, s	
group	system	[NaCl], M	→	←	→	←
c/c	PMANa/PEVP(500)	0.05	7.1 ± 0.5	7 ± 1	35 ± 3	38 ± 4
		0.10	18 ± 2	24 ± 2	<5	<5
	PS-*b*-PMANa/PEVP(500) + PMANa	0.10		31 ± 2	27 ± 1	
c/m	PS-*b*-PEVP/PMANa + PMANa	0.10			43 ± 10	34 ± 10
		0.10	13 ± 1	13 ± 1	1100 ± 200	6000 ± 3000
	PS-*b*-PMANa/PEVP(500)	0.05	4 ± 1	4 ± 1	2500 ± 1000	6500 ± 1000
m/m	PS-*b*-PANa/PEVP(500)	0.10	12 ± 4	11 ± 2	5000 ± 1000	6000 ± 1000
	PS-*b*-PMANa/PEVP(1900)	0.10	1.6 ± 0.4	2.4 ± 0.8	24000 ± 10000	32000 ± 20000

[a] pH 10; $[COO^-] = [COO^-]^* = 5 \times 10^{-4}$ M. "→" indicates "direct" reaction; "←" indicates "reverse" reaction; c, coil; m, micelle.

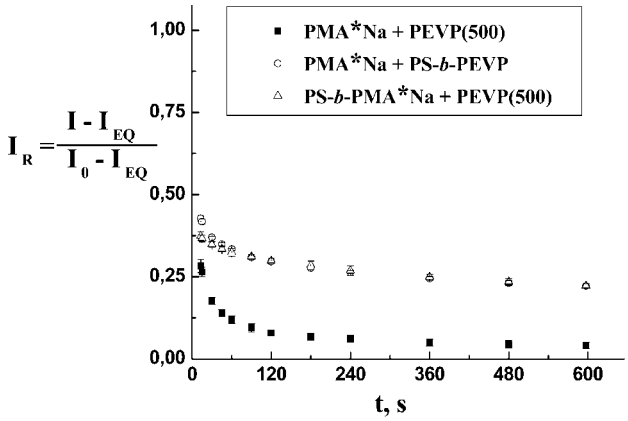

Figure 3. Kinetic curves (reduced fluorescence intensity vs time) for polyion coupling reactions. [NaCl] = 0.01 M; pH 10 (adjusted by NaOH); $[COO^-]^* = 1 \times 10^{-3}$ M; $[Py^+] = 3 \times 10^{-4}$ M.

equivalent to mutual penetration of a linear PMANa coil and PMANa shell of the {PS-*b*-PMANa/PEVP} BICs. Therefore, it is not surprising that corresponding coil/micelle reaction rates are similar.

Polyion Coupling Reactions. The polyion coupling at an excess of anionic polymeric component $Z = [Py^+]/[COO^-] = 0.3$ resulted in the formation of soluble IPECs or BICs. We compared (i) the IPEC formation as a result of coupling of two linear polyions, PMA*Na and PEVP, with the BIC formation as a result of coupling of (ii) PS-*b*-PMA*Na micelles and PEVP (PSM excess) or (iii) PMA*Na and PS-*b*-PEVP micelles (polyanion coils excess). In these cases, the reduced fluorescence intensity was expressed as follows: $I_R = (I - I_{EQ})/(I_0 - I_{EQ})$, where I, I_o, and I_{EQ} are the fluorescence intensities of the mixture at any given time, the free polyion ($Z = 0$), and the equilibrated complex ($Z = 0.3$), respectively (Figure 3). (In this case, $I_R = 1$ at the initial mixing point and then gradually decreases to 0 upon equilibration.)

The data on the polyion coupling reactions reinforced the same conclusion that was achieved for the polyion interchange: reactions involving PSM were much slower than similar reactions involving the polyion coils (Figure 3). For example, the coupling reaction of two linear polyions reached equilibrium within 300 s (curve 1), whereas the coupling reaction between linear and micelle polyions did reach $I_R \approx 0.25$ within 600 s (curves 2 and 3). Coupling reactions between the two PSM of opposite charge were not investigated because the product was an insoluble complex.

It is well-known that the coupling reaction between two linear polyions involves two stages.[30] The first stage is the reproaching of polyions that leads to nonequilibrium complex formation. This stage proceeds within milliseconds, that is, during the mixing of the components and is accompanied with a sharp decrease of a relative fluorescence (not seen in the figure). The second slower stage is the formation of equilibrium complexes through polyion interchange reactions[30] (stage is reflected in the kinetic curves in Figure 3). Therefore, it is not surprising that the processes involving PSM are slower than those involving polyion coils.

Conclusion

This study demonstrates that self-assembly of amphiphilic ionic block copolymers into multimolecular PSM decreases the rates of the polyion interchange and coupling reactions compared to similar reactions involving single polyion coils. This phenomenon is especially pronounced in cases when the polyion reaction involves a stage of mutual penetration of two micelles. The decrease of the reaction rate is most likely due to high ionic group and polyion chain density in the micelle shells which decreases the efficiency of the shells interpenetration due to electrostatic and steric repulsion. The phenomenon observed may permit construction of delivery systems with prolonged action and, in combination with earlier described factors (such as ionic strength, polyion length, charge density, etc.), provide an additional tool for tuning the drug release rates in BIC-based drug delivery systems. Altogether these studies present new information on dynamic properties of BIC that can find useful application in plarmaceutics and nanopharmacology.

Acknowledgment. The authors acknowledge the support to this work provided by the USA National Science Foundation (DMR-0513699), Russian Basic Research Foundation (RFBR) (Grant No 06-03-32964-a), joint RFBR-NSF program (Grant No 06-03-90153-NSF-a), and Canadian National Science and Engineering Research Council (STR-0181003). We thank Dr. Xing Fu Zhong (McGill University), who synthesized and characterized the block copolymers in connection with other projects. We also thank Prof. Alexander Zezin (Moscow State University) for fruitful discussions.

References and Notes

(1) Kabanov, A. V.; Vinogradov, S. V.; Suzdaltseva, Yu. G; Alakhov, V. Yu *Bioconjugate Chem.* **1995**, *6*, 639–643.
(2) Harada, A.; Kataoka, K. *Macromolecules* **1995**, *28*, 5294–5299.
(3) Smid, J.; Fish, D. Polyelectrolyte Complexes. In *Encyclopedia of Polymer Science and Engineering*; Mark, H. F. , Bikales, N. M. , Overberger, C. G. , Menges, G. , Eds.; Wiley: New York, 1988; Vol. 11, p 720.
(4) Kabanov, V. Fundamentals of Polyelectrolyte Complexes in Solution and the Bulk. In *Multilayer Thin Films*; Decher, G. , Schlenoff, J. B., Eds.; Wiley-VCH: Weinheim, Germany, 2003; p 47.
(5) Thünemann, A. F.; Müller, M.; Dautzenberg, H.; Joanny, J-F.; Löwen, H. *Adv. Polym. Sci.* **2004**, *166*, 113–171.
(6) Selb, J.; Gallot, Y. Ionic Block Copolymers. In *Developments in Block Copolymers*; Goodman, I. , Ed.; London: Elsevier Applied Science, 1985; Vol. 2, p 27.
(7) Zhang, L.; Khougaz , K.; Moffitt, M.; Eisenberg, A. Self-Assembly of Block Polyelectrolytes. In *Amphiphilic Block Copolymers: Self-Assembly and Application*; Alexandridis, P., Lindman , B., Eds.; Amsterdam, The Netherlands: Elsevier, 2000, p 87.
(8) Kabanov, A. V.; Kabanov, V. A. *Adv. Drug Delivery Rev.* **1998**, *30*, 49–60.
(9) Nguyen, H. K.; Lemieux, P.; Vinogradov, S. V.; Gebhart, C. L.; Guerin, N.; Paradis, G.; Bronich, T. K.; Alakhov, V. Y.; Kabanov, A. V. *Gene Ther.* **2000**, *7*, 126–138.
(10) Tang, G. P.; Zeng, J. M.; Gao, S. J.; Ma, Y. X.; Shi, L.; Li, Y.; Too, H.-P.; Wang, S. *Biomaterials* **2003**, *24*, 2351–2362.
(11) Putnam, D.; Zelikin, A. N.; Izumrudov, V. A.; Langer, R. *Biomaterials* **2003**, *24*, 4425–4433.
(12) Talingting, M. R.; Voigt, U.; Munk, P.; Webber, S. E. *Macromolecules* **2000**, *33*, 9612–9619.
(13) Pergushov, D. V.; Remizova, E. V.; Feldthusen, J.; Zezin, A. B.; Müller, A. H. E.; Kabanov, V. A. *J. Phys. Chem. B* **2003**, *107*, 8093–8096.
(14) Pergushov, D. V.; Remizova, E. V.; Gradzielski, M.; Lindner, P.; Feldthusen, J.; Zezin, A. B.; Müller, A. H. E.; Kabanov, V. A. *Polymer* **2004**, *45*, 367–378.
(15) Burkhardt, M.; Ruppel, M.; Tea, S.; Drechsler, M.; Schweins, R.; Pergushov, D. V.; Gradzielski, M.; Zezin, A. B.; Müller, A. H. E. *Langmuir* **2008**, *24*, 1769–1777.
(16) Chelushkin, P. S.; Lysenko, E. A.; Bronich, T. K.; Eisenberg, A.; Kabanov, A. V.; Kabanov, V. A. *Dokl. Phys. Chem.* **2004**, *395*, 72–75.
(17) Lysenko, E. A.; Chelushkin, P. S.; Bronich, T. K.; Eisenberg, A.; Kabanov, V. A.; Kabanov, A. V. *J. Phys. Chem. B* **2004**, *108*, 12352–12359.
(18) Matejicek, P.; Uchman, M.; Lokajova, J.; Stepanek, M.; Prochazka, K.; Spirkova, M. *J. Phys. Chem. B* **2007**, *111*, 8394–8401.
(19) Chelushkin, P. S.; Lysenko, E. A.; Bronich, T. K.; Eisenberg, A.; Kabanov, V. A.; Kabanov, A. V. *J. Phys. Chem. B* **2007**, *111*, 8419–8425.
(20) Wittemann, A.; Ballauff, M. *Phys. Chem. Chem. Phys.* **2006**, *8*, 5269–5275.
(21) Zintchenko, A.; Rother, G.; Dautzenberg, H. *Langmuir* **2003**, *19*, 2507–2513.

(22) Holappa, S.; Kantonen, L.; Andersson, T.; Winnik, F.; Tenhu, H. *Langmuir* **2005**, *21*, 11431–11438.

(23) Li, Y.; Bronich, T. K.; Chelushkin, P. S.; Kabanov, A. V. *Macromolecules* **2008**, 41. submitted for publication.

(24) Zhu, J.; Eisenberg, A.; Lennox, R. B. *J. Am. Chem. Soc.* **1991**, *113*, 5583–5588.

(25) Lysenko, E. A.; Bronich, T. K.; Slonkina, E. V.; Eisenberg, A.; Kabanov, V. A.; Kabanov, A. V. *Macromolecules* **2002**, *35*, 6351–6361.

(26) Zhong, X. F.; Varshney, S. K.; Eisenberg, A. *Macromolecules* **1992**, *25*, 7160–7167.

(27) Adamczyk, M.; Fino, L.; Fishpaugh, J. R.; Johnson, D. D.; Mattingly, P. G. *Bioconjugate Chem.* **1994**, *5*, 459–462.

(28) Zakharova, J. A.; Otdelnova, M. V.; Ivleva, E. M.; Kasaikin, V. A.; Zezin, A. B.; Kabanov, V. A. *Polymer* **2007**, *48*, 220–228.

(29) One notable exception is BICs formed by double hydrophilic block copolymers containing polyion and nonionic water-soluble chains.[1, 2] Such BICs self-assemble into micelles with a polyion complex core and nonionic polymer shell, which can be stable in aqueous dispersion even at stoichiometric composition upon complete neutralization of charges.

(30) Bakeev, K. N.; Izumrudov, V. A.; Kuchanov, S. I.; Zezin, A. B.; Kabanov, V. A. *Macromolecules* **1992**, *25*, 4249–4254.

(31) Kabanov, V. A.; Zezin, A. B.; Izumrudov, V. A.; Bronich, T. K.; Bakeev, K. N. *Makromol. Chem., Suppl.* **1985**, *13*, 137–155.

(32) Such analysis is valid because all complexes showed linear dependence of I on the complex composition within the range $0 \leq Z \leq 0.3$ (data not shown).

(33) Notably, the fluorescence quenching in the {PEVP/PS-*b*-PMANa} + PS-*b*-PMA*Na system cannot not be explained by exchange of PS-*b*-PMA*Na chains between free micelles and BIC particles, since according to ref 34, such exchange is prohibited for PS-*b*-PMAA micelles in aqueous media. In other words, changes in fluoresce intensity in these systems are caused only by reaction II.

(34) Tian, M.; Qin, A.; Ramireddy, C.; Webber, S. E.; Munk, P.; Tuzar, Z.; Prochazka, K. *Langmuir* **1993**, *9*, 1741–1748.

(35) The average concentration of ionic groups $[\text{ionic groups}]_{\text{shell}}$ was calculated as $X_{\text{ionic}}N_w/[4/3N_A\pi R_h^3\ 10^{-24} - M_{PS}N_wX_{PS}/(1000\rho)]$, where X_{ionic} is the polymerization degree of the ionic block, X_{PS} is the polymerization degree of the PS-block, N_A is Avogadro's number, $M_{PS} = 104$ g/mol is the molar mass of the PS unit, $\rho = 1.04$ g/cm^3 is the density of polystyrene in a bulk, and R_h is expressed in nanometers.

(36) Guenoun, P.; Davis, H. T.; Tirrell, M.; Mays, J. W. *Macromolecules* **1996**, *29*, 3965–3969.

JP8012877